Inorg. Chem. **2007**, *46*, 7528–7535

On the Mechanism of Triclinic Distortion in Chevrel Phase as Probed by In-Situ Neutron Diffraction

E. Levi,*,† A. Mitelman,† D. Aurbach,† and O. Isnard‡,§

Department of Chemistry, Bar-Ilan University, Ramat-Gan, Israel 52900, Institut Néel CNRS, associé à l'Université J. Fourier, BP166X, 38042 Grenoble Cedex 9, France, Institut Laue Langevin, BP 156 X, 38042 Grenoble Cedex 9, France

Received May 4, 2007

This work presents, for the first time, a general mechanism of a rhombohedral (R)–triclinic (T) phase transition in Chevrel Phases (CPs) with small cations (radius < 1 Å), which was unclear in spite of intensive studies of these important materials in the past. In contrast to previous interpretation of the R ⇔ T transition in some CPs as cation ordering, T-distortion is regarded here as a particular case of general adaptation of the framework to cation insertion, which includes the deformations of the coordination polyhedra and their tilting. The research is based on a combination of experimental studies (in-situ neutron diffraction at different temperatures) for one model compound, $MgMo_6Se_8$, and structural analysis for a variety of known CPs. This analysis shows that the structure flexibility is fundamentally different for the R and T forms. As a result of the lower flexibility, in the R form, a strict correlation exists between the compression of the framework along the –3 symmetry axis and the cation position in the structure (the so-called 'delocalization'). The decreasing delocalization in the R-CPs, which occurs on cooling, leads to excessive repulsion within the cations pairs (R-$Cu_{1.8}Mo_6S_8$ case) or undesirable asymmetry in the cation polyhedra (R-$MgMo_6Se_8$ case). The higher flexibility of the T framework allows for relaxation of these structural strains by increasing the cation–cation distances and forming a more symmetric cation environment, sometimes with higher coordination number (CN), like CN = 5 in the T-$Fe_2Mo_6S_8$ type. Thus, this work also proposes possible driving forces for T-distortion in CPs.

Introduction

Chevrel Phases (CPs), $M_xMo_6T_8$ (M = metal, T = S, Se, Te), were intensively studied since the 1970s because of their unusual superconducting, magnetic, and thermoelectric properties.[1−4] In addition, unusually high mobility of various mono- and divalent cations found for Mo_6T_8 (T = S, Se) hosts[5−9] make possible the use of these material as unique cathodes for rechargeable Mg batteries.[10−13] Our previous studies, devoted to the phase diagram of Mg insertion into Mo_6T_8, were focused on the correlation between the cation mobility and some peculiarities of the CPs' crystal structure.[12,14,15] Moreover, these studies brought us to the question about the mechanism of triclinic distortion in the CPs.

The CPs, especially these with "small cations", crystallize in two major modifications: rhombohedral (R) and triclinic (T).[1,2,16−20] Both of them can be described as a stacking of

* To whom correspondence should be addressed. E-mail: elenal@mail.biu.ac.il.
† Bar-Ilan University.
‡ Institut Néel CNRS.
§ Institut Laue Langevin.

(1) Yvon, K. In *Current Topics in Material Science*; Kaldis, E., Ed.; Elsevier: North-Holland, Amsterdam 1979; Vol. 3.
(2) *Topics in Current Physics: Superconductivity in Ternary Compounds I*; Fisher, Ø., Maple, M. B., Eds.; Springer-Verlag: Berlin 1982.
(3) Brorson, M.; King, J. D.; Kiriakidou, K.; Prestopino, F.; Nordlander, E. *Met. Clusters Chem.* **1999**, *2*, 741.
(4) Nunes, R. W.; Mazin, I. I.; Singh, D. *J. Phys. Rev. B* **1999**, *59*, 7969.
(5) Schöllhorn, R. *Angew. Chem., Int. Ed. Engl.* **1980**, *19*, 983.
(6) Fischer, C.; Gocke, E.; Stege, U.; Schöllhorn, R, *J. Solid-State Chem.* **1993**, *102*, 54.
(7) Tarascon, J. M.; Hull, G. W.; Marsh, P.; Ter Haar *J. Solid State Chem.* **1987**, *66*, 204.
(8) Gocke, E.; Schramm. W.; Dolscheid, P.; Schöllhorn, R. *J. Solid-State Chem.* **1987**, *70*, 71.
(9) Schöllhorn, R.; Kumpers. M.; Besenhard, J. O. *Mat. Res. Bull.* **1977**, *12*, 781.
(10) Aurbach, D.; Lu, Z.; Schechter, A.; Gofer, Y.; Gizbar, H.; Turgeman, R.; Cohen, Y.; Moskovich, M.; Levi, E. *Nature* **2000**, *407*, 724.
(11) Aurbach, D.; Gofer, Y.; Lu, Z.; Schechter, A.; Chusid, O.; Gizbar, H.; Cohen, Y.; Ashkenazi, V.; Moskovich, Turgeman, R.; Levi, E. *J. Power Sources* **2001**, *97*, 28.
(12) Aurbach, D.; Weissman, I.; Gofer, Y.; Levi, E. *Chem. Record* **2003**, *3*, 61.
(13) Levi, M. D.; Lancry, E.; Levi, E.; Gizbar, H.; Gofer, Y.; Aurbach, D. *Solid-State Ionics* **2005**, *176*, 1695.

10.1021/ic7008573 CCC: $37.00
Published on Web 07/28/2007

Mo_6T_8 blocks with pseudo-cubic cavities available for cation accommodation. According to the literature data,[1,2,16−18] the R and T forms differ mainly in the cation arrangement. For instance, cations in R-$Cu_{1.8}Mo_6S_8$[16] are distributed statistically between six equivalent tetrahedral positions (forming the so-called inner ring). In contrast, in T-$Cu_{1.8}Mo_6S_8$,[17] only two of the six tetrahedra are occupied by cations. This pair of sites linked by an inversion center is called a dumbbell.[1,2,17]

The R→T phase transition usually occurs on cooling, and thus, in the classic reviews[1,2] it was interpreted as "freezing" of the formerly mobile cations in fixed positions. The "freezing" model is based on two ideas: (1) a direct correlation between the cation mobility in CPs and the crystal symmetry and (2) order−disorder character of the phase transition.

However, both of these postulates seem to be questionable. First of all, in general, the "frozen" cations that lost their mobility can be distributed statistically between the same six equivalent sites, maintaining R symmetry. In the same way, the mobile cations may occupy only two of the six sites, resulting in T symmetry. Thus, the correlation between the cation mobility and the CPs' symmetry is not obvious. Concerning the second suggestion, more recent works[14,19,20] showed that the occupation of the dumbbell sites in T-CPs might have a statistic character, just as with the R-CPs. For instance, in triclinic $MgMo_6Se_8$,[14] a single Mg^{2+} cation is distributed randomly between two equivalent positions connected to each other by the inversion center −1. A disordered cation distribution was found also in T-$Ni_{0.85}Mo_6Te_8$.[21] Thus, one cannot be certain that the cation ordering is really a typical characteristic feature of the R→T phase transition in the CPs.

In the most detailed work,[22] devoted to the lattice instability of CPs, Yvon suggested a possible correlation between cation position (so-called "delocalization") and T-distortion (more detailed description of delocalization will be done in the Result and Discussion section). He showed that the delocalization or the cation shift from a single potential well, as well as the character of the phase transition, depends mainly on the cation radius. Transitions for CPs with large localized cations are of a magnetic origin. For CPs with small, delocalized cations, it was mentioned that the Mo_6T_8 units remain intact and change only their relative orientation during T-distortion. According to Yvon, the latter transformations evoke ordering of the cations at low temperature. However, this idea of the changes in the linkage of the Mo_6T_8 units was not illustrated or advanced. Moreover, a driving force of the T-distortion remained unclear: Actually, displacive phase transitions may proceed without ordering.[23] Thus, more careful analysis of structural changes is needed to clarify the character of the R→T phase transition in CPs with small cations.

In our previous work,[14] it was established that $MgMo_6Se_8$ is triclinic at room temperature but rhombohedral at 300 °C. The transition temperature, as well as the structural parameters for the R form, was not determined, but, as will be shown below, its crystal structure is similar to that of classic CPs with small cations. Thus, the square-pyramidal anion coordination around Mg^{2+} cations found for the T form[14] (T-$Fe_2Mo_6S_8$ structural type) transforms to a tetrahedron in the R form. Such pronounced structural change makes $MgMo_6Se_8$ a good model compound for studying the mechanism of the phase transition. $MgMo_6Se_8$ should be even better than $Fe_2Mo_6S_8$ because in the former case the specific interactions between Mo and the inserted cations can be excluded (the influence of the M−Mo interactions (M = 3d elements), which appear as short M−Mo distances, on the CPs crystal structure was discussed in refs 19, 20).

The aim of the present work was to clarify the mechanism of the T→R transition for CPs with small cations. First, high-resolution neutron diffraction at high temperature (300 °C) was used to determine the crystal structure of R-$MgMo_6Se_8$. By in-situ neutron diffraction, we followed the structural changes ensued by heating T-$MgMo_6Se_8$. The temperature of the phase transition and its deformational character were established. At the second stage, a geometric approach was used to analyze the deformations in the main structural blocks of known CPs and their tilting. In this analysis, T-distortion was regarded as a particular case of the general adaptation of the Mo_6T_8 framework to cation insertion. Special attention was devoted to (i) correlation between the deformations and the cation delocalization, (ii) the flexibility of the framework in R- and T-CPs, and (iii) the role of the flexibility and the cation delocalization in the symmetry adoption.

Experimental Section

$MgMo_6Se_8$ was prepared at 650 °C by heating Mg powder and binary Mo_6Se_8 in an evacuated, sealed, quartz tube for a week. In order to prevent Mg from reacting with the quartz, a corundum crucible inside the tube was used. To ensure the desirable stoichiometry of the product after its air stabilization, the Mg concentration in the initial mixture was 1.5 times higher than that in the intended formula, $MgMo_6Se_8$.[14]

The neutron diffraction experiments were performed at the Institut Laue Langevin (I.L.L.) at Grenoble, France. The high-resolution powder diffractometer D1A was used for analysis of the crystal structure at 27 and 300 °C, while the in-situ measurements were carried out with the high-flux D1B instrument. A detailed description of these instruments is available via the Internet at http://www.ill.fr. D1B and D1A are powder diffractometers operating with the takeoff angle of the monochromator at 44° and 122° (in 2θ), respectively. In the configuration used, the resolution of D1B was about 0.3° (fwhm) at 80° (in 2θ). The measurements were carried out at a wavelength of $\lambda = 1.911$ (D1A) and 2.52 (D1B) Å selected by the (115) reflection of a germanium and the (002) reflection of a pyrolitic graphite monochromators, respectively.

(14) Levi, E.; Lancry, E.; Mitelman, A.; Aurbach, D.; Isnard O.; Djurado D, *Chem. Mater.* **2006**, *18*, 3705.
(15) Levi, E.; Lancry, E.; Mitelman, A.; Aurbach, D.; Ceder, G.; Morgan, D.; Isnard, O. *Chem. Mater.* **2006**, *18*, 5492.
(16) Yvon, K.; Paoli, A.; Flukiger, R.; Chevrel, R. *Acta Crystallogr. B* **1977**, *33*, 3066.
(17) Yvon, K.; Baillif, R.; Flukiger, R. *Acta Crystallogr. B* **1979**, *35*, 2859.
(18) Yvon, K.; Chevrel, R.; Sergent, M. *Acta Crystallogr. B* **1980**, *36*, 685.
(19) Roche, C.; Chevrel, R.; Jenny, A.; Pecheur, P.; Scherrer, H.; Scherrer, S. *Phys. Rev. B* **1999**, *60*, 16442.
(20) Mancour-Billah, A.; Chevrel, R. *J. Solid-State Chem.* **2003**, *170*, 281.
(21) Hoenle, W.; Yvon, K. *J. Solid-State Chem.* **1987**, *70*, 235.
(22) Yvon, K. *Solid-State Comm.* **1978**, *25*, 327.
(23) Dove, M. T. *Am. Mineral.* **1997**, *82*, 213.

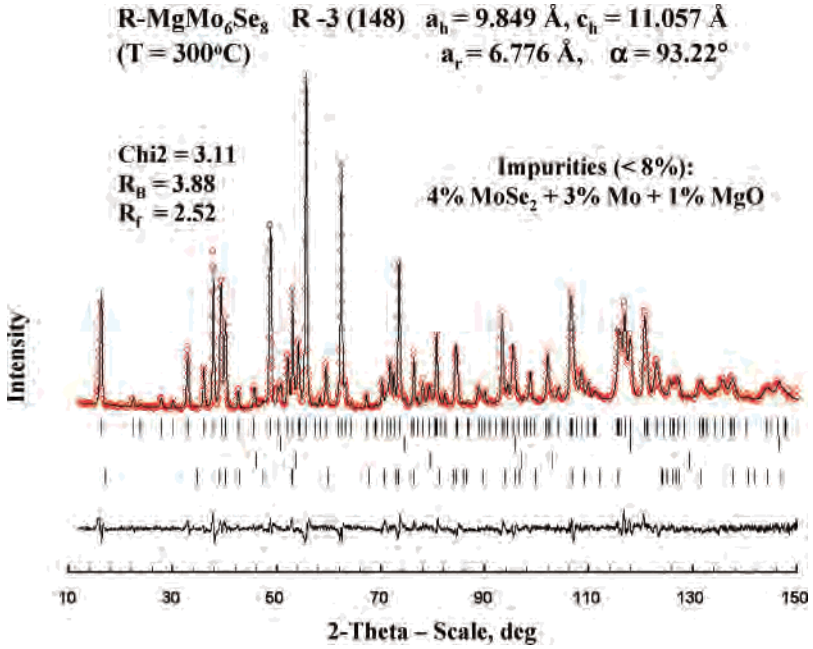

Figure 1. Neutron Rietveld profile for R-$MgMo_6Se_8$. The calculated 2θ values of the reflections (vertical bars) correspond to R-$MgMo_6Se_8$, Mo, MgO, and $MoSe_2$ (top-down).

Diffraction data were collected over the angular ranges of $3° < 2\theta < 151°$ and $20° < 2\theta < 100°$, step sizes 0.05° and 0.2° for D1A and D1B, respectively. A vanadium cylinder of 7 mm inner diameter was used as a sample holder. The measurements on the two-axis diffractometer D1B were performed with a 400 cell ^{3}He multidetector covering the range of 80° in 2θ. On the D1A instrument, neutron detection was achieved with a set of 25 ^{3}He counting tubes (6° spaced). The complete diffraction pattern was obtained by scanning over the whole 2θ range.

The data were analyzed by the Rietveld structure refinement program FULLPROF.[24] The Thompson−Cox−Hastings pseudo-Voigt function was used for the peak-shape approximation. The background was refined by a polynomial function. Agreement factors used in this article are defined according to the guidelines of the Rietveld refinement that can be found elsewhere.[25] The neutron scattering lengths used were b_{Se}=0.7970 10^{-14} m, b_{Mg}=0.5375 10^{-14} m, and b_{Mo} = 0.6715 10^{-14} m, values taken from ref 26.[26]

Results and Discussion

Crystal Structure of High-Temperature $MgMo_6Se_8$. As was mentioned above, $MgMo_6Se_8$ is triclinic at room temperature (space group $P\bar{1}$, a = 6.743 Å, b = 6.755 Å, c = 6.761 Å, α = 91.22°, β = 94.29°, γ = 94.44°) but rhombohedral at 300 °C (space group $R\bar{3}$, $a_r = 6.75 \pm 0.02$ Å, $\alpha = 93.1° \pm 0.2°$).[14] The data for the T form were obtained previously by Rietveld analysis on the basis of the combined powder X-ray and high-resolution neutron diffraction, while the unit cell parameters of the R form were determined by relatively short-time X-ray measurements in a high-temperature camera.[14] The unit cell parameters, obtained in the latter experiments, were used as the initial ones for the Rietveld analysis in this work.

Table 1. Comparison between Atomic Coordinates in the Crystal Structures of R-$Cu_2Mo_6Se_8$ (25 °C)[1] and R-$MgMo_6Se_8$ (300 °C)

compound	atom Wyck	x	y	z	occ
R-$Cu_2Mo_6Se_8$	Mo 18f	0.0162	0.1625	0.3955	1
R-$MgMo_6Se_8$		0.0162(3)	0.1658(3)	0.3975(3)	1
R-$Cu_2Mo_6Se_8$	Se_1 18f	0.3162	0.2807	0.4089	1
R-$MgMo_6Se_8$		0.3219(3)	0.2857(2)	0.4121(3)	1
R-$Cu_2Mo_6Se_8$	Se_2 6c	0	0	0.2050	1
R-$MgMo_6Se_8$		0	0	0.2147(3)	1
R-$Cu_2Mo_6Se_8$	Cu1 18f	0.795	0.413	0.334	0.16
R-$MgMo_6Se_8$	Mg 18f	0.774(2)	0.392(4)	0.345(2)	0.151(4)

Figure 1 presents the fitting of the neutron diffraction pattern recorded for the R form at 300 °C. The atomic positions in the initial model were identical to that of R-$Cu_2Mo_6Se_8$.[1] The atomic displacement parameters obtained in the refinement of $MgMo_6Se_8$ were 1.05(5) Å^2 for Mo and 1.3(1) Å^2 for Se, while for Mg this parameter held constant and equal to 1 Å.[2] Tables 1 and 2 compare the atomic coordinates and the interatomic distances, respectively, for these two compounds. The CN of the Mg^{2+} cation in R-$MgMo_6Se_8$ is equal to 4 (tetrahedral coordination). The bond valence sum, calculated for the Mg^{2+} ion, is equal to 1.97. As can be seen, the crystal structure of the high-temperature form of $MgMo_6Se_8$ can be described as classic CP with small cations.

Structural Parameters of $MgMo_6Se_8$ Measured upon the T→R Phase Transition. Figure 2a presents the neutron diffraction profiles (diffractometer D1B) obtained for $MgMo_6Se_8$ at different temperatures. The change of the symmetry can be easily observed by the temperature evolution of the diffraction pattern, in particular in the following 2θ ranges: 65−75° and 85−90°. The T→R phase transition takes place near 80 °C, while the refinement does not show the co-

(24) Rodriguez Carjaval, J. *Physica B* **1993**, *192*, 55.
(25) McCusker, L. B.; Von Dreele, R. B.; Cox, D. E.; Louer, D.; Scardi, P. *J. Appl. Crystallogr.* **1999**, *32*, 36.
(26) Sears, V. F. *Neutron News* **1992**, *3*, 26.
(27) Belin, S.; Chevrel, R.; Sergent, M. *J. Solid-State Chem.* **2000**, *155*, 250.

Table 2. Interatomic Distances in R-$MgMo_6Se_8$ (Å)

distance	R-$MgMo_6Se_8$ (300 °C)	R−$Cu_2Mo_6Se_8$ (25 °C)
Mo−Mo	2.701(5)	2.680
	2.751(5)	2.727
	3.451(3)	3.491
Mo−Se	2.553(4)	2.551
	2.556(4)	2.565
	2.589(4)	2.579
	2.633(4)	2.616
	2.663(4)	2.673
Mo−Mg1 (Cu1)	3.69(3)	3.53
Mo−Mg2 (Cu2)	−	3.12
Mg1 (Cu1)−Se	2.43(2)	2.464
	2.59(3)	2.477
	2.59(3)	2.498
	2.67(2)	2.501
	3.33(4)	3.545
Se−Se	3.656 ± 0.005	3.65[a]
	(3.524 ÷ 3.758)[a]	

[a] Mean value of the nine shortest distances.

existence of T and R phases. Figure 2b compares the neutron diffraction patterns of the T and R forms for two temperatures (55 and 99 °C). As usual, the T→R phase transition results in fewer diffraction peaks of higher intensity.

The lattice parameters of the R and T forms at different temperatures obtained by the Rietveld refinement are presented in Figure 3. As expected, cooling leads to decreasing in the unit cell dimensions for the R form. Surprisingly, after the R→T phase transformation, the cell volume increases with cooling, but this increase takes place over a relatively small temperature range, from 78 to 63 °C. A similar increase in the unit cell dimensions after the R→T phase was found for $Cu_{1.8}Mo_6S_8$.[16] For $MgMo_6Se_8$, below 63 °C, the cell volume decreases again upon cooling. The identical unit cell parameters of the R form become anisotropic in the T form, but this change occurs very gradually and affects mainly the angles.

R ⇔ T Phase Transition as a Particular Case of the Mo_6T_8-Framework Adaptation to Cation Insertion (Deformational Mechanism). Approach to the Problem. According to the results presented above, it can be suggested that the triclinic distortion in $MgMo_6Se_8$ has a deformational character. Thus, in order to clarify the mechanism of the T-distortion in CPs, we have to map what kinds of deformations are typical for the CPs crystal structure, what are the possible reasons for these deformations, and how these deformations correlate with the symmetry of CPs.

As was mentioned in the Introduction section, the most known features of the R→T phase transition in CPs is the transformation of the inner ring of the cation sites to a dumbbell,[1,2] while previous analysis of deformations was limited to the changes in the unit cell parameters.[16] The question arises about the convenience of the latter presentation to describe the distortion mechanism. Figure 4 presents the deviations of the lattice parameters for known T-CPs from their average values, $a_{av} = 1/3\ (a + b + c)$ and $\alpha_{av} = 1/3\ (\alpha + \beta + \gamma)$. The latter can be considered as unit cell parameters of imaginary undistorted R forms of the same compounds (the structural data for these compounds were found in refs 14, 17−19, 28). One can see that, in spite of the similar variations in the angles of the T cell (α and β are chosen as the largest and the smallest angles, respectively), it is difficult to find correlation in the changes of the *a*, *b*, and *c* parameters for different compositions. The reason is that in many cases the deformations in the main structural blocks and their tilting compensate each other. As a result, the variations in the dimensions of the larger structural blocks, like unit cells, are useless for pursuing the effect of T-distortion on the geometry of the structure.

In our work we used the so-called 'geometric approach' to the phase transitions known for silicates, perovskites and other minerals (see, for instance, the review in ref 23 and the references therein). This approach is based on the polyhedral-tilting model and focuses on matching between rigid structural elements, e.g., between $[MO_6]$ cation octahedra and $[SiO_4]$ tetrahedra. Both polyhedra are rigid, and the matching is achieved owing to the flexibility of the silicate framework. In the latter, a loose junction of the tetrahedra allows for their tilting and rotation. It was shown that such an approach is very useful in elucidation of structural transformations in these materials, but it was never used for CPs.

Deformations in the Crystal Structures of the R-CPs. In the context of the geometric approach, our first task was to choose the main structural elements of the CPs, as well as to understand the limits of their rigidity and flexibility of their link. Figure 5a presents the linkage of the main structural elements in the crystal structure of R-CPs. As can be seen, in contrast to common ionic compounds, the CPs crystal structure cannot be presented as a close packing of anions, but rather as a framework of anion pseudo-cubes. Hence, the main structural elements of the CPs are Mo_6T_8 blocks and pseudo-cubic cavities, but for the latter, we can restrict our analysis only to deformations of the pseudo-cubic cavity 1. In fact, the dimensions of cavities 2 and 3 are not independent because they are linked to cavities 1 and to the Mo_6T_8 blocks by common faces.

Moreover, as can be seen in Figure 5a and b, two anions, T_2, lie on the −3 axis, while six others anions (T_1) form a "pleated" ring around this axis. As a result of such an arrangement, the cubes can be compressed or elongated only along its diagonals (Figure 5c presents a schematic mechanical model of such deformations along and normal to the −3 axis). Thus, for the R-CPs we used the relative differences between two diagonals of the cubes, $\Delta d/d = (d_c - d_a)/d_c$ and $(\Delta d/d)' = (d'_c - d'_a)/d'_c$, to characterize their deformations.

Figure 6 presents the deformations of the cubes and their tilt, namely the angle between diagonals d_a and d'_a, vs cation delocalization for a variety of known R-CPs (the angle between the diagonals d_c and d'_c is constant and equal to 180° because both diagonals lie on the −3 axis). As can be seen, the tilting angles for different R-CPs are very similar and close to 135° because of the strong intercluster interactions.[1,2] In contrast, a strict correlation exists between the compression of the framework along the −3 symmetry axis and the cation position in the crystal structure: The cation

(28) Harbrecht, B.; Mahne, S. J. *Alloys Compounds* **1992**, *178*, 467.

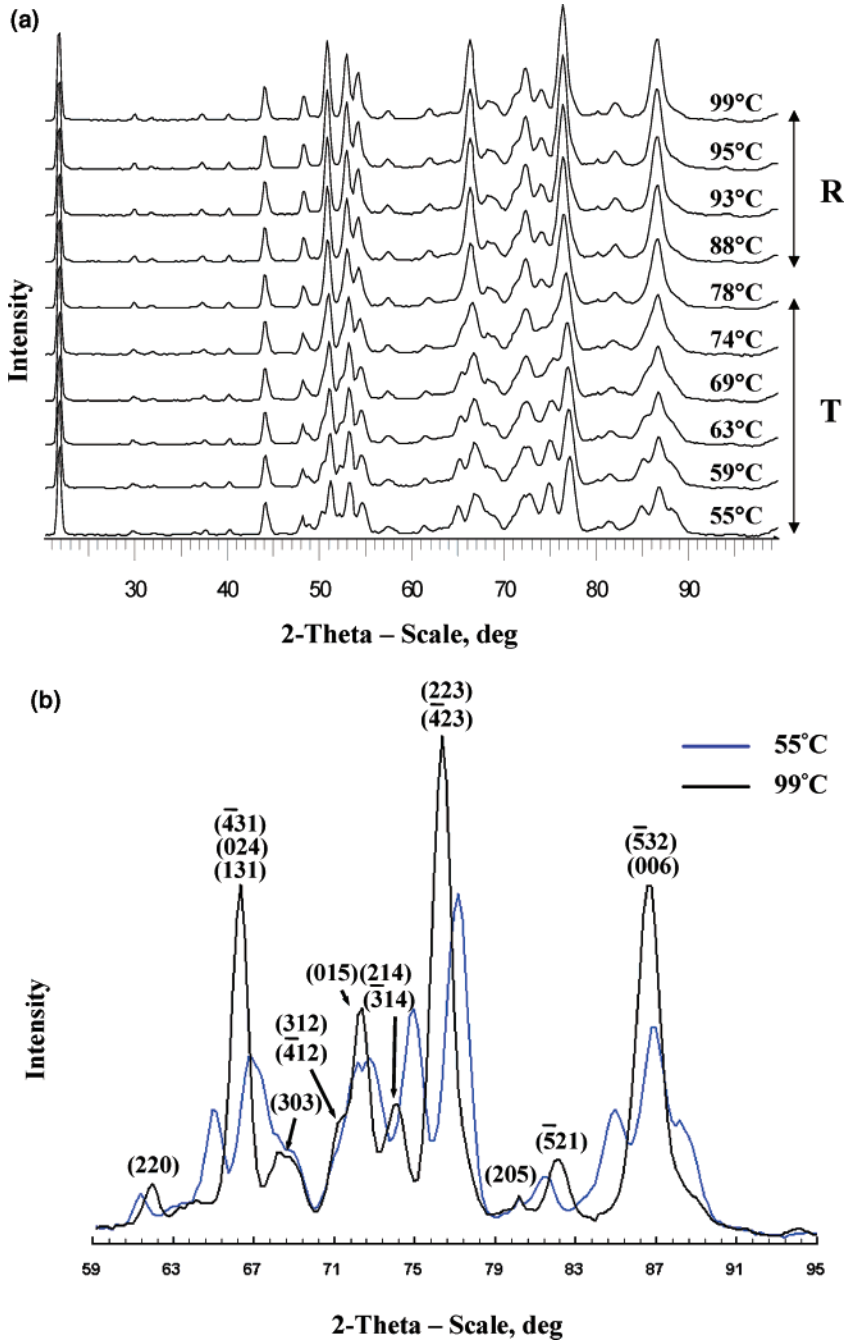

Figure 2. In-situ neutron diffraction profiles for $MgMo_6Se_8$: (a) series of scans in the temperature range from 55 to 99 °C; (b) two scans for 55 and 99 °C with typical changes of the patterns related to the phase transition.

delocalization is accompanied by an increasing squeezing of cavity 1 and elongation of the Mo_6T_8 block along the −3 axis, but the distortion of the latter is effectively smaller than that of cavity 1, i.e., this block is much more rigid. Thus, the flexibility of the R form is provided mostly by the deformation of cavity 1.

Deformations in the Crystal Structure of T-CPs. In the T forms all four diagonals of the pseudo-cubes and the angles between them may be different because T symmetry allows for the anisotropy of deformations in all directions. Figure 7 shows the basic difference in the linkage of the structural blocks in the R and T forms related to their symmetry: In the R form the diagonals d_c of cavity 1 and d'_c of the Mo_6T_8 blocks lie on the same direct line (−3 symmetry axis). In contrast, in T-CPs there is some tilting of the main structural blocks, i.e., the angle α_c between these diagonals is always smaller than 180°. Such a linkage results in additional flexibility of the framework because its deformations in this direction may be caused not only by variation in the diagonals of the structural elements but also by changes in the angles α_c.

Figure 8 presents the relative differences in the angles $\Delta\alpha_i/\alpha_i$, as well as the deformations in the main structural blocks for known CPs, which crystallize in the T and R forms at different temperatures ($MgMo_6Se_8$ and $Cu_{1.8}Mo_6S_{8)}$, or change their symmetry with variation of the chemical compositions ($Fe_xMo_6S_8$ for $x = 1.3$, 2 and $Ni_xMo_6Se_8$ for $x = 0.7$, 1.2). As in the previous case, these deformations were defined as the relative differences between corresponding

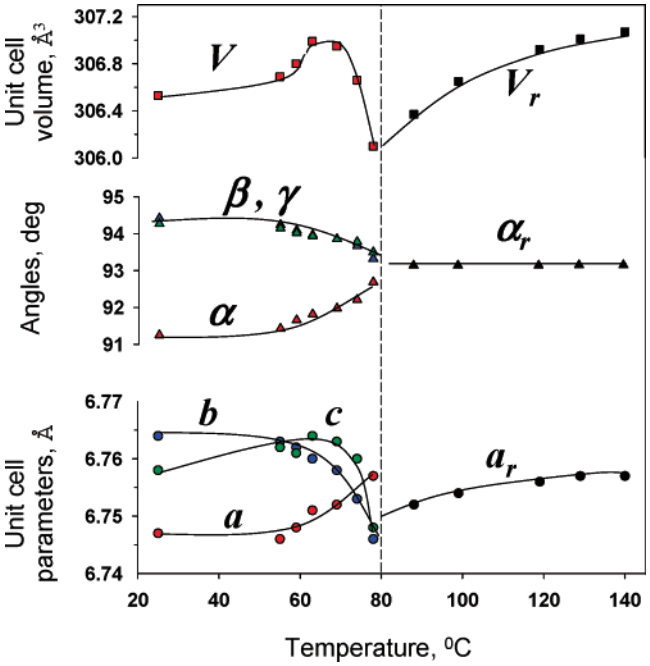

Figure 3. Lattice parameters of the R and T forms of $MgMo_6Se_8$ at different temperatures.

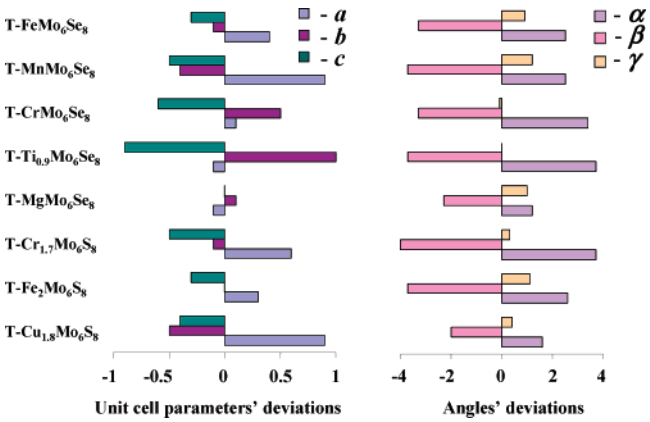

Figure 4. Deviations in the lattice parameters of known T-CPs from their average values.

diagonals. Directions *X*, *Y*, and *U*, which are equivalent for R-CPs, become different for T-CPs (Figure 9).

As can be seen (Figure 8), a T-distortion results in a slight shrinkage of cavity 1 in the *Y*, *U*, and *Z* directions (along the former −3 axis), as well as in the clear expansion in the *X* direction. These changes can be compensated or increased by variations in the dimensions of the Mo_6T_8 blocks and the corresponding angles. For instance, in the *U* direction, the simultaneous decrease of the diagonals of cavity 1 and the angles results in a more evident compression of the framework related to the T-distortion. It can be shown (see Supporting Information) that other T-CPs have similar values of the diagonals and tilting angles.

Thus, we can suggest that the crystal structures of all the T-CPs are the result of the same type of gentle deformations described above. Actually, in spite of the more flexible character of the Mo_6T_8 framework in the T form as compared to the R form, its deformation ability is limited by intercluster interactions that keep the framework from more significant

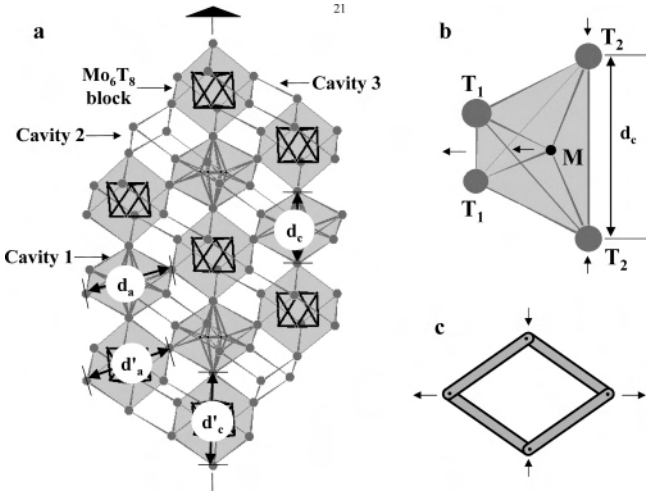

Figure 5. (a) Linkage of the main structural elements (Mo_6T_8 blocks and pseudo-cubic cavities) in the crystal structure of R-CPs; (b) orientation of the $[MT_4]$ tetrahedron (M-cation site) relative to the cavity 1′ diagonal that follows the −3 symmetry axis. The arrows show the typical deformations associated with the decrease of the cation size; (c) schematic "mechanical" model of the deformations along and normal to the −3 axis.

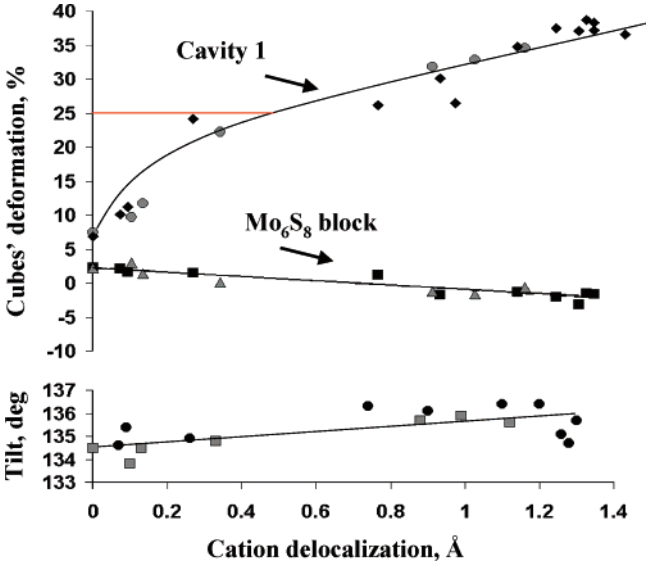

Figure 6. Deformations of the main structural elements and their tilt in known R-CPs (sulfides and selenides) vs cation delocalization. The red line shows the squeezing of cavity 1 in pure Mo_6S_8 and Mo_6Se_8.

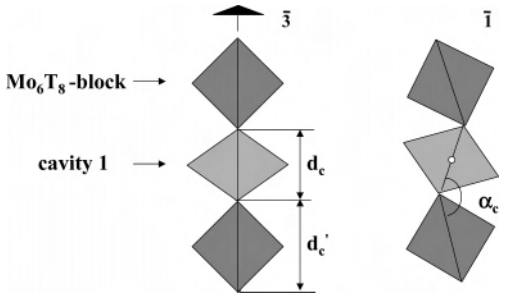

Figure 7. Basic difference in the linkage of the main structural elements of the R and T forms related to their symmetry.

changes. Unusually high deformations take place only in the crystal structure of $Cu_4Mo_6Se_8$ (see Supporting Information). They are related to the absence of the intercluster bonding for two of the six Mo atoms in each cluster and the exceptional cation positions in the common faces of cavities

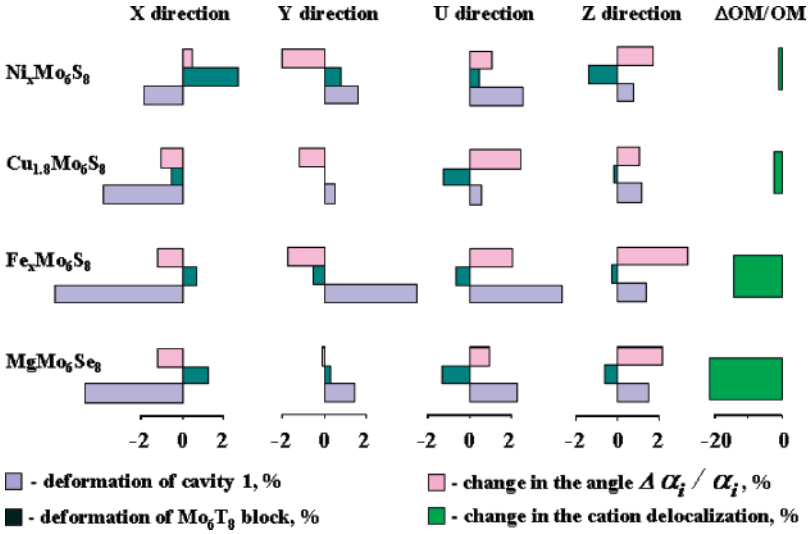

Figure 8. Changes in the crystal structure of CPs related to T-distortion.

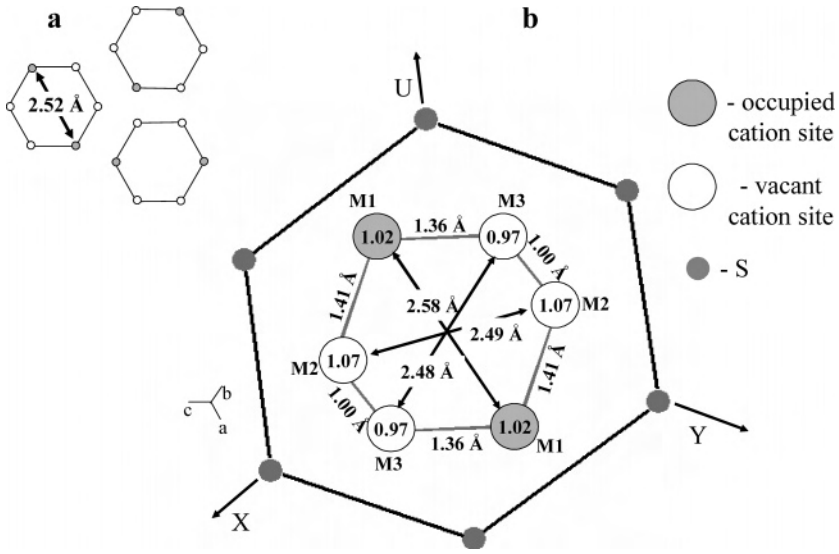

Figure 9. Difference in the cations distribution between the R and T forms of $Cu_{1.8}Mo_6S_8$: (a) A random distribution of Cu−Cu pairs in the inner rings of sites for R-$Cu_{1.8}Mo_6S_8$. (b) The map of the cation sites in cavity 1 for T-$Cu_{1.8}Mo_6S_8$. Projection (111). The values inside the circles are the bond valence sums for these sites.

2 and 3.[29] Interestingly, only the changes in the *Z* direction in this compound are not in accordance with the common compression of cavity 1. The deformations in other directions have the same tendency as in other CPs.

Figure 8 shows also that T-distortion is accompanied by a clear increase in cation delocalization, OM, which is especially high for the Mg^{2+} ions (the latter values present the relative difference in the cation delocalizations for the R and T forms of the same compound). It seems that this result is crucial for understanding the driving force of the phase transition in this type of CPs. Actually, in the previous works[1,2] it was shown that the cation position in CPs depends mainly on its size. Moreover, according to Yvon,[1] cooling results in lower cation delocalization. This effect for R-$MgMo_6Se_8$ in the temperature range 310−88 °C is rather small and close to the precision of our measurements (0.99 and 0.88 Å for 310 and 88 °C, respectively). However, the smaller squeezing of cavity 1 at 88 °C as compared to that at 310 °C (see Supporting Information) confirms this result. Thus, the increase in the cation delocalization for lower temperature should have some important reason, which may be at the same time a possible reason of the phase transition. Below we present some examples that illustrate the role of cation delocalization and the framework flexibility in the symmetry adoption of the CPs.

T-Distortion in $Cu_xMo_6S_8$. As was mentioned in the Introduction, the idea of T-distortion as cation ordering was based on the studies of this material. Thus, it seems important to revise our knowledge about its crystal structure. In contrast to most CPs, $Cu_xMo_6S_8$ allows for the presence of two cations in cavity 1.[1,2,16] It is commonly accepted that in the R form these cations are statistically distributed between six equivalent sites, but it should be emphasized that the distribution of the two cations is not independent. In fact, the distances between the adjacent cation sites of the same ring are too short (1.12 Å). As a result, the only possible arrangement

(29) McGuire, M. A.; Ranjan, C.; DiSalvo, F. J. *Inorg. Chem.* **2006**, *45*, 2718.

for the cations is simultaneous occupancy of two opposite sites within the ring. Even in this case the distance between these two cations (double value of the cation delocalization) in R-$Cu_{1.8}Mo_6S_8$ at RT is rather small (2.52 Å) and evident of special metallic interactions between these cations. Thus, the Cu−Cu pairs in cavity 1 exist not only in the T form but also in the R form. The only difference is that in the R form the relative orientation of such pairs changes randomly from one inner ring to another (Figure 9a) while in the T form it is the same for all the crystal structure (Figure 9b).

In order to recognize the driving force for the T-distortion in the material, it is important to recall that cooling results in a decrease of the cation delocalization in R-CPs. This decrease cannot be avoided because, as was shown above, the deformations in the rigid R-CPs framework are strictly correlated to the cation shift from the center of cavity 1. Thus, cooling R-$Cu_{1.8}Mo_6S_8$ down to the transition temperature should result in an extremely short Cu−Cu distance (less than 2.52 Å). It can be suggested that the transformation of the structure occurs when the repulsion between two Cu^+ cations reaches a critical value. This suggestion seems logical because after the phase transition, the Cu−Cu distance increases up to 2.58 Å, owing to the higher flexibility of the Mo_6T_8 framework in the T form. The energetic gain related to the phase transition, should exceed the increase of the cell volume found for $Cu_{1.8}Mo_6S_8$.[17]

T-Distortion in $MgMo_6Se_8$ and $FeMo_6S_8$. As was shown in this paper, the crystal structure of $MgMo_6Se_8$ at elevated temperatures (>80 °C) is identical to that of R-$Cu_{1.8}Mo_6S_8$, but in contrast to the latter, only one Mg^{2+} cation is distributed statistically between six equivalent sites of the inner ring. Actually, the distance between the opposite sites of the inner ring for R-$MgMo_6Se_8$ (88 °C) is too short (1.76 Å) to allow formation of Mg−Mg pairs. Thus, the cation repulsion cannot be responsible for the phase transition in $MgMo_6Se_8$. Moreover, in spite of the basic similarity of the R forms for these compounds, their T forms have different cation coordination: tetrahedral for $Cu_{1.8}Mo_6S_8$ and square pyramidal for $MgMo_6Se_8$[14] (like in $FeMo_6S_8$[18]). In the previous parts we discussed the geometry of pseudo-cubic cavity 1 as entire block. Now, let us look more carefully at the environment of individual cations.

The most astonishing feature of coordination polyhedra around cations in the CPs, as compared to oxides or other close-packed ionic compounds, is their strong distortion. It can be shown that the asymmetry of [MT_4] tetrahedra in R-CPs increases for cations with smaller delocalization, and it is especially high for R-$MgMo_6Se_8$ (Figure 10). This asymmetry should be in conflict with the character of the Mg^{2+} ion, namely with its tendency to form symmetric ionic bonding with anions. Thus, it can be suggested that the R→T phase transition in $MgMo_6Se_8$ occurs when decreasing cation delocalization on cooling reaches some critical value. For the latter compound, as well as for $FeMo_6S_8$, T-distortion allows for the relaxation of the strains caused by cooling and formation of more symmetric bonding with higher CN. As in the case of $Cu_{1.8}Mo_6S_8$, the energetic gain related to the phase transition should exceed the increase in the cell volume, which was found for $MgMo_6Se_8$ after its T-distortion.

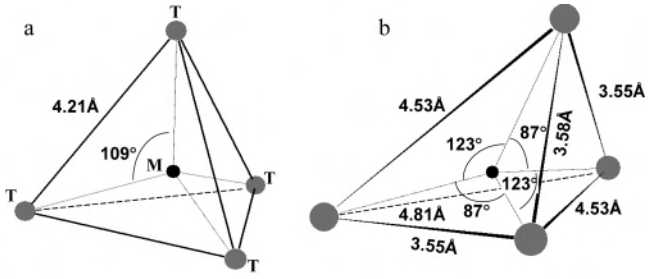

Figure 10. Dimensions of the [MT_4] tetrahedra in R-$MgMo_6Se_8$: (a) ideal case, (b) real case at 88 °C.

These examples show that the phase transition in CPs occurs when the rigid R framework is unable to ensure desirable cation−cation interactions (e.g., a formation of Cu−Cu pairs) or anion environment appropriated for inserted cations. The latter can be achieved only by the more flexible T structure, which presents also more rich variety of the cation sites.

Conclusions

A general mechanism of T-distortion in CPs with small cations was presented for the first time by a combination of in-situ neutron diffraction at different temperatures for the model material, $MgMo_6Se_8$, and structural analysis for a variety of known compounds. In contrast to previous interpretation of the R→T transition in some CPs as cation ordering, T-distortion was regarded in this work as a particular case of general adaptation of the framework to cation insertion, which includes the deformations of the coordination polyhedra and their tilting.

It was shown that the structural flexibility is fundamentally different for the R and T forms. As a result of the lower flexibility in the R form, a strict correlation exists between the compression of the framework along the −3 symmetry axis and the cation position in the structure ('delocalization'). The decreasing delocalization in the R-CPs, on cooling, leads to excessive repulsion within the cation pairs (R-$Cu_{1.8}Mo_6S_8$) or undesirable asymmetry of the cation polyhedra (R-$MgMo_6Se_8$). The higher flexibility of the T framework allows for relaxation of these structural strains by increasing the cation−cation distances and forming a more symmetric cation environment, sometimes with higher CN (e.g., CN = 5 in T-$Fe_2Mo_6S_8$ and T-$MgMo_6Se_8$).

Acknowledgment. Partial support for this work was obtained from the Israel−U.S. binational foundation (B.S.F.). The Institut Laue Langevin is warmly acknowledged for providing the neutron facilities.

Supporting Information Available: Crystallographic information in the form of a cif file, lattice parameters of T-CPs and their deviations from the average values in the form of a table, and deformations in the main structural elements and their tilt in R and T-CPs vs cation delocalization in the form of tables. This material is available free of charge via the Internet at http://pubs.acs.org.

IC7008573